Early dynamics of the emission of solvated electrons from nanodiamonds in water

Franziska Buchner,[1] Thorren Kirschbaum,[1,2] Amélie Venerosy[3], Hugues Girard,[3] Jean-Charles Arnault,[3] Benjamin Kiendl,[4] Anke Krueger,[4,5] Karin Larsson,[6] Annika Bande,[1] Tristan Petit,[1,*] Christoph Merschjann[1,*]

[1] Helmholtz-Zentrum Berlin für Materialien und Energie GmbH, Hahn-Meitner-Platz 1, 14109 Berlin, Germany
[2] Freie Universität Berlin, FB Mathematik & Informatik, Artificial Intelligence for the Sciences, Arnimallee 12, D-14195 Berlin, Germany
[3] Université Paris-Saclay, CEA, CNRS, NIMBE, 91191 Gif sur Yvette Cedex, France
[4] Institut für Organische Chemie, Julius-Maximilians-Universität Würzburg, Am Hubland, D-97074 Würzburg, Germany
[5] Wilhelm-Conrad Röntgen Research Center for Complex Materials (RCCM), Julius-Maximilians-Universität Würzburg, Am Hubland, D-97074 Würzburg, Germany
[6] Uppsala University, Lägerhyddsvägen 1, 751 21, Uppsala, Sweden

E-Mail: tristan.petit@helmholtz-berlin.de, christoph.merschjann@helmholtz-berlin.de

Abstract

Solvated electrons are among the most reductive species in aqueous environment. Diamond materials have been proposed as a promising source for solvated electrons, but the underlying emission process in water remains elusive so far. Here, we show spectroscopic evidence for the emission of solvated electrons from nanodiamonds upon excitation with both deep ultraviolet (255 nm) and visible (400 nm) light using ultrafast transient absorption. The crucial role of surface termination for the emission process is evidenced by comparing hydrogenated, hydroxylated and carboxylated nanodiamonds. Especially, hydrogenated nanodiamonds are able to generate solvated electron upon visible light excitation, while they show a sub-ps recombination due to trap states when excited with deep ultraviolet light. The essential role of surface reconstructions on the nanodiamonds in these processes is proposed based on density functional theory calculations. These results open new perspectives for solar-driven emission of solvated electrons in aqueous phase using nanodiamonds.

Keywords: diamond, nanoparticles, solvated electron, surface chemistry, transient absorption

1 Introduction

Solvated electrons are highly reductive chemical species involved in many reactions from radiochemistry to photocatalysis.[1] Different sources have been considered for the emission of solvated electrons from ionic precursors,[2] metals,[3–5] metal oxides[6] or diamond surfaces.[7] Diamond materials are particularly interesting due to the negative electron affinity (EA) of the diamond surface when terminated with hydrogen atoms, enabling a spontaneous and barrier-free electron emission once electrons are excited into the conduction band.[8] Especially, diamond has been used to trigger chemical reduction of nitrogen or carbon dioxide directly in the aqueous phase using electrochemical reaction[9,10] or light excitation.[11,12] The latter represents a great challenge due to the large bandgap of diamond of 5.5 eV, necessitating the use of deep ultraviolet (DUV) light, which is absent from the solar spectrum.[11] So far, clear evidence of the light-induced emission of solvated electrons from diamond in water is scarce. Electron emission was recently shown for hydrogenated nanodiamonds (NDs) in aqueous suspensions under X-ray irradiation.[13] Indirect demonstration were provided on boron doped diamond electrodes,[7,14] NDs[15] and silver-doped diamond thin films.[16] In a seminal work, Zhu *et al.* demonstrated that upon DUV light excitation, a transient signal at 633 nm was observed in water above a diamond single crystal which was assigned to solvated electrons.[7] It was recently completed by a detailed study of transient absorption in the ns-µs range, showing sub-bandgap electron emission for excitation down to 4.5 eV (275 nm).[14] Nevertheless, the time evolution over the early stages (< 2 ns) of the electron emission under DUV light remains unexplored to our knowledge. Achieving electron emission with visible (VIS) light excitation instead of DUV light would also be required for a larger significance of diamond in the field of photocatalysis.

A promising strategy to achieve solvated electron emission with VIS light consists in adding new electronic states within the bandgap of the diamond material that can be excited with VIS photons above the diamond conduction band maximum (CBM). Several strategies were employed to achieve sub-bandgap absorption, including dye sensitization,[17] plasmonic coupling,[16] nanostructuring[18] and doping.[19,20] The main challenge is to keep the electron emission properties offered by H-terminated surfaces while modifying the diamond material properties. Sub-bandgap visible absorption with diamond materials was previously reported in vacuum[20,21] but remains to be shown in water. Visible-light reactivity toward CO_2 photoelectrochemical reduction was recently demonstrated on hydrogenated nanostructured diamond surface by some of us.[22] The origin of enhanced reactivity with visible light remains elusive so far. Thus, identifying electron emission processes involved in sub-bandgap (visible) excitation would certainly facilitate the design of more efficient diamond-based electron emitters.

In this study, we have employed ultrafast transient absorption (TA) spectroscopy with sub-ps time resolution to monitor the early stages of solvated electron emission from detonation NDs in water. Aqueous dispersions of NDs with hydrogenated (ND-H), carboxylated (ND-COOH) and hydroxylated (ND-OH) surface were compared. The impact of excitation photon energy was studied by applying both DUV (225 nm, 5.5 eV) and VIS (400 nm, 3.1 eV) pump laser pulses. All ND surface terminations were found to enable the emission of solvated electrons with DUV light. Furthermore, a substantial solvated electron emission was observed for ND-H under visible light. Based on these TA measurements and density functional theory (DFT) calculations, possible mechanisms for the emission of solvated electrons in DUV and VIS regions are proposed.

2 Results and Discussion

The surface chemistry of ND-H, ND-OH and ND-COOH was first characterized by FTIR, showing the efficient hydrogenation of ND-H after plasma treatment and hydroxylation of ND-OH after reduction of carboxyl and carbonyl groups (see SI and Figure S1 for details). The ultrafast response of NDs under light excitation is probed by TA experiments based on a pump-probe scheme where an aqueous ND dispersion is excited by a pump laser pulse and the absorption change in the visible and near-infrared (NIR) range (500-950nm) is monitored in transmission geometry, using a white light probe pulse (see ref. [23] and the SI for details). The time-dependent information is obtained by delaying the probe pulse with respect to the pump pulse, thus measuring the absorption change at different delay times. The delay between the two pulses was adjusted up to 30 ps with an effective temporal resolution of approximately 150 fs (determined by the pulse durations of the pump and probe pulse, respectively). DUV pump pulses were applied to induce the emission of solvated electrons from ND dispersions via a direct bandgap excitation. In a second set of experiments, VIS light excitation was used to investigate the possibility to emit solvated electrons from NDs in water via sub-bandgap absorption. Sodium iodide (NaI) solution was used as an ionic source of solvated electrons, for which the solvation dynamics has been extensively studied.[2,24–26]

Figure 1 shows time-dependent TA spectra for ND-H (**a**, **b**) and NaI (**c**, **d**) solutions, both under DUV (**a**, **c**) and VIS (**b**, **d**) excitation, respectively. Note the semilogarithmic time axis as well as the different absolute signals for the different measurements. In the case of DUV excitation, the probe range is limited to the range 500-750 nm due to the different probe light generation scheme (see SI). The signal obtained for NaI is similar to previously reported studies.[2] For both excitation scenarios, ND-H exhibits a clear positive transient signal at positive delay times. As observed for VIS excitation, the TA signal peaks around 750 nm after about 1 ps, similarly to NaI. The blue shift of the TA maximum throughout the first 1 ps observed for NaI cannot be clearly distinguished for ND-H. The 2D TA traces for the other ND samples are available in the SI (Figure S3). In general, the acquired TA spectra are broad and featureless for NDs, and substantially weaker than for NaI solutions. Therefore, we concentrate in the following on the temporal profile of the integrated TA response, which provides more information on the dynamics of the electron emission process.

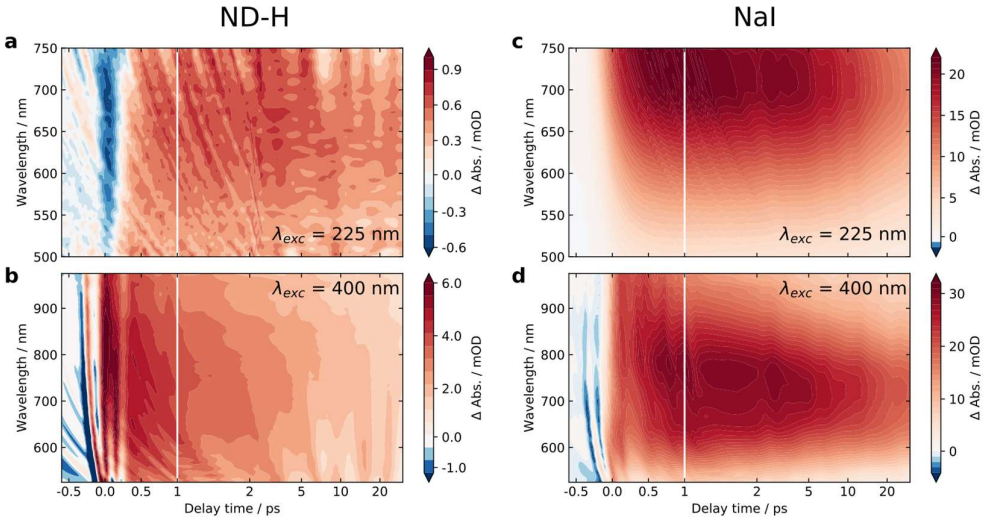

Figure 1 Transient absorption (TA) spectra of aqueous solutions of H-terminated nanodiamonds and NaI solution. **a, b**, TA signal from ND-H dispersion as a function of probe wavelength and delay time for DUV (**a**) and visible (**b**) excitation. **c, d**, TA signal from NaI as a function of probe wavelength and delay time for DUV (**a**) and VIS (**b**)

excitation. Note the semilogarithmic time axis as well as the different absolute signals. The negative absorbance change around zero delay time in **a** is discussed in the main text, while the oscillatory features in **b, d** are due to cross-phase modulation, induced by the comparably strong VIS pump pulse.

The integrated TA traces over the probe wavelength region of 600 - 740 nm for ND-H, ND-OH and ND-COOH under DUV excitation are shown in *Figure 2***a**. For ND-H, a strong negative TA signal around time zero is observed, which is absent in NaI solution, pure water, and for the other NDs characterized with similar pump laser intensity (Figure S2 and S3). The origin of this additional ultrafast process on ND-H will be discussed in the following. After about 1 ps, a positive signal reaches a maximum and slowly decays over the probed timescale of 30 ps. For ND-OH and ND-COOH, a strong increase of the TA signal occurs in the first 500 fs and it progressively decays similarly to ND-H. The kinetics in the first 2 ps and the subsequent decay appear generally faster for the NDs than for NaI, with minor differences between the surface terminations. Due to the observed similarities of both the spectral and temporal features with NaI, we assign the positive TA signals in the ND dispersions to the emission of solvated electrons upon DUV excitation. The emission of solvated electrons is therefore observed from all surface terminations after DUV excitation above the diamond bandgap.

Slight temporal differences are observed between ND-OH and ND-COOH, which are likely related to different solvation of the emitted electron in the first picoseconds. Both terminations have indeed opposite zeta-potential,[27] which suggest a different organization of the first hydration shell impacting the electron solvation. In general, the more ordered water hydration structure observed around NDs[27] may lead to faster kinetics compared to solvated electrons emitted from iodide. The early dynamics was also found to be faster on detonation NDs compared to larger NDs synthesized from High Pressure High Temperature (HPHT) synthesis for carboxylated surfaces (Figure S4). Even though solvated electrons are detected from ND-OH or ND-COOH under DUV light, oxidized diamond surfaces have previously shown much lower photocatalytic activity than hydrogenated diamond surfaces.[7] This can be explained by a surface-dependent diamond-water band alignment as detailed below.

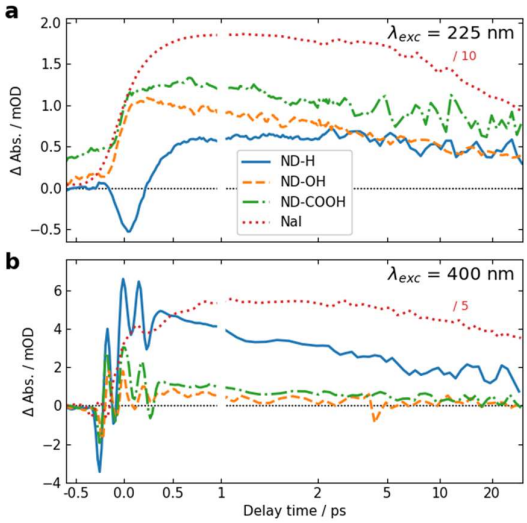

Figure 2 TA traces for NDs, surface-terminated with hydrogen (ND-H), hydroxyl (ND-OH), and carboxyl (ND-COOH), respectively. **a**, Delay-dependent TA signals for DUV excitation, averaged over a probe wavelength region of 600 - 740 nm. For comparison, the TA signal obtained from NaI solution is shown as dashed red line (note the demagnification factor). **b**, Same as **a**, but for VIS excitation. Note the semilogarithmic time axis.

For VIS excitation, an analogous treatment of the 2D TA maps is shown in *Figure 2***b**. Compared to the previously used DUV pulses, the VIS pump light contains around 70 times more photons per pulse, which leads to a pronounced and complex coherent artefact also observed for pure water (Figure S2). Apart from that, the spectro-temporal behavior for NaI solution under VIS excitation appears quite similar to that under DUV excitation. For NDs, two notable differences are found compared to DUV excitation. Firstly, no negative TA can be observed for any of the samples, especially not for ND-H. Secondly, a substantial positive TA signal after the initial ultrafast time range is only observable for ND-H. Similar to the DUV excitation, the kinetics in ND-H are slightly faster than in the respective NaI solution.

We interpret the different behavior of ND-H compared to ND-OH and ND-COOH (further referred to as ND-O) for both DUV and VIS excitation by distinct electron emission processes summarized in *Figure 3*. First of all, surface termination is affecting the diamond electron affinity (EA).[8] The EA of (111) diamond surfaces terminated with hydrogenated and hydroxylated surfaces were calculated in vacuum and with a thin water film using DFT calculation (see SI). While both surfaces were found to have a negative EA in vacuum (-1.0 eV for H-termination and -0.4 eV for OH-termination), only the H-terminated surface maintains a negative EA with a thin adsorbed water film at neutral pH (-0.3 eV for H-termination and +0.7 eV for OH-termination). A positive EA is also expected for strongly oxidized diamond surfaces.[8]

Despite its positive EA, the electron emission is possible for ND-O because the water CBM most likely sit below the CBM of ND-O as illustrated in *Figure 3*. The surface termination of NDs strongly influences the orientation of the first water solvation shells via the strength of the hydrogen bonds.[27] Such interfacial water layers will also modify the EA of the water layer adsorbed on the ND surface. Previous DFT calculations have indeed shown that the bulk EA of water (0.2 eV) is different from surface water close to a vacuum interface (0.8 eV).[28] In any case, the electron emission from hydrogen-terminated diamond is more efficient due to the larger energy difference between diamond and water CBM, ensured by a negative EA, as well as the possibility to emit electrons through surface C-H states.[14] Nevertheless, the H-terminated surface alone cannot explain electron emission upon VIS excitation, as it would only allow electron emission for excitation with photon energies above 4.5 eV.[14] Another absorption process must therefore take place on ND-H upon VIS excitation.

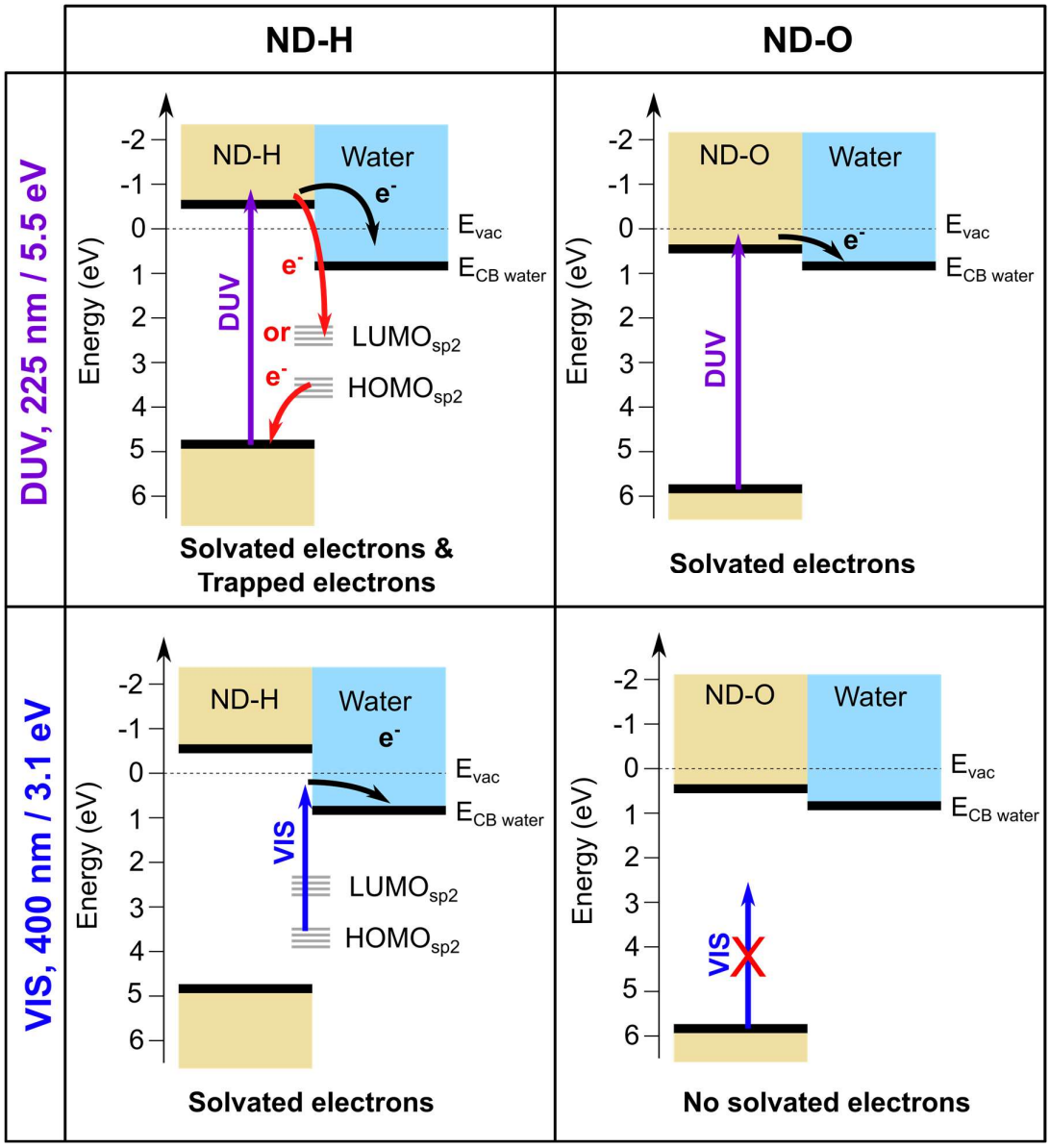

Figure 3 Schematic representation of solvated electron emission process on ND-H and ND-O for DUV and VIS light excitation. ND-O refers to either ND-OH or ND-COOH for simplification. The HOMO and LUMO of sp^2-hybridized surface states on ND-H are indicated in grey.

The negative ultrafast TA signal only observed for the ND-H under DUV illumination suggests that an additional process occurs for ND-H during the first picosecond. It could be due either to stimulated emission or a ground-state bleach of a species to be identified. It turns out that the surface termination of ND-H is not only composed of CH_x groups but also contains small sp^2 graphitic islands.[29] Recent sp^2 carbon quantification based on near-edge X-ray absorption fine structures (NEXAFS) on NDs hydrogenated, either by plasma or by annealing treatments, have concluded that up to 20% of the carbon atoms may be sp^2-hybridized, predominantly those situated at the ND surface.[30] These sp^2-hybridized carbon are mostly localized on fullerene-like reconstructions (FLRs) which were also identified on NDs annealed in vacuum.[31] These non-diamond carbon atoms induce new states below the CBM of ND-H, which contribute to visible light absorption and were found to increase significantly the photoluminescence of ND-H, compared to oxidized surfaces. [30,32]

To quantify the energy levels of an sp^2-decorated ND, we performed hybrid-DFT calculations on a series of ND structures with various degrees of FLRs coverage. The structures were optimized by tight-binding DFT[33] and subsequent single point calculations were performed on PBE0-D3/SVP level of theory. The corresponding structures and their orbital energies are depicted in *Figure 4*.

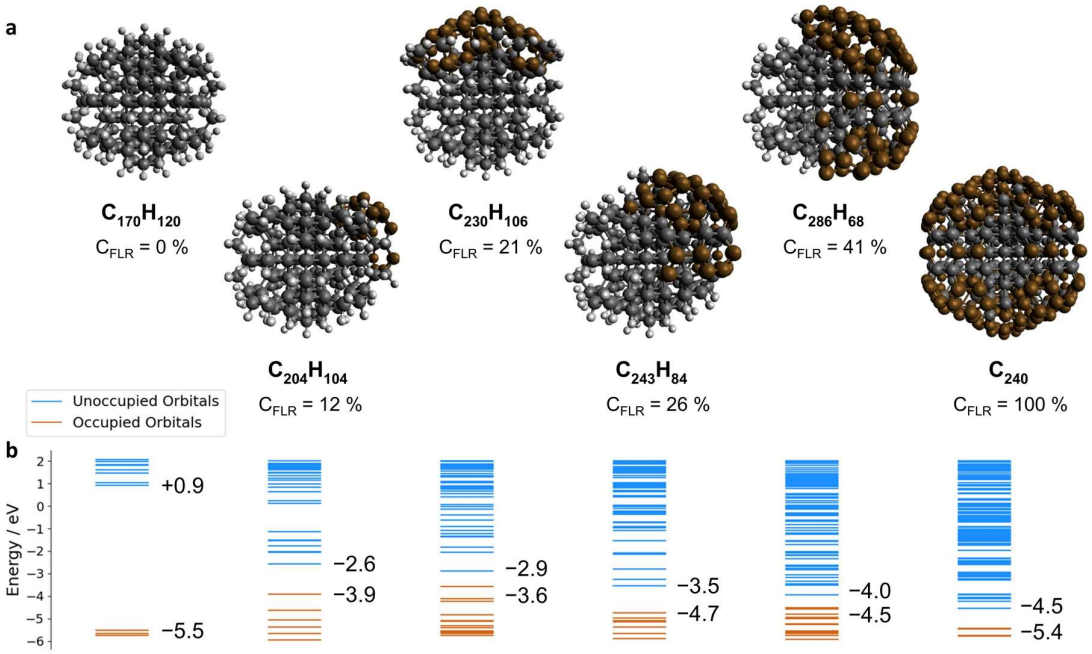

Figure 4 (a) Structures, sum formulae and FLR coverage (C_{FLR}, atom %) of the ND series. (b) Energy diagram of the occupied and unoccupied orbitals from the structures in (a). The HOMO and LUMO energies are given. From left to right: ND-H $C_{170}H_{120}$, sp^2-decorated NDs $C_{240}H_{104}$, $C_{230}H_{106}$, $C_{243}H_{84}$, $C_{286}H_{68}$, and fully surface graphitized ND C_{450}. sp^3 carbon atoms are depicted in black, sp^{3-x} (x>0) carbon atoms in brown, hydrogen atoms in light grey.

The ND-H has a negative electron affinity of −0.93 eV, which is similar to the calculation performed on H-terminated (111) diamond, and a HOMO-LUMO gap (HLG) of 6.46 eV. This HLG is higher than the bandgap of bulk diamond (5.5 eV) due to the quantum confinement effect present on small ND.[34] Upon addition of sp^2 carbon on the ND, the frontier orbital energies are shifted upwards (HOMO) and downwards (LUMO), resulting in decreased HLGs. These frontier orbitals and the next few highest occupied/lowest unoccupied orbitals of the NDs partially covered by FLRs are all located on the respective sp^2-hybridized carbon areas. Contour plots of the relevant orbitals are shown in the SI. With increasing FLRs coverage, additional orbitals are present within the range of the ND-H's HLG. Interestingly, the HOMO energies are highest with a low amount of FLRs present and decrease with increasing reconstructed areas. This decrease of HOMO energies is, however, not monotonous. In contrast, the systems' LUMO energies decrease monotonously with increasing FLRs coverage. We further computed optical absorption spectra of smaller NDs with 0, 50 and 100 at% surface reconstruction, each surrounded by an explicit layer of water molecules (SI). The spectra confirm that the optical gap of a H-terminated ND is also significantly reduced upon surface reconstruction.

These findings support the fact that sub-bandgap states are introduced in NDs upon formation of FLRs on their surface, and even a small coverage (e.g., 12 % of surface atoms) is sufficient to introduce them. The additional unoccupied surface states may act as trap states that, upon DUV excitation, induce ultrafast recombination of the excited electrons

which is detrimental to the solvated electron emission as illustrated in the *Figure 3*. An alternative process may be recombination of electrons from an occupied surface state with valence band holes in the excited ND. In either case, the electrons coming from fully H-terminated areas on the ND-H surface may not be affected by these defect states and are then emitted into the water. As a result, the ultrafast TA response of the ND-H dispersion upon DUV excitation consists of two parallel processes: (i) a strong recombination at early dynamics due to defect states and (ii) the emission of solvated electrons from fully hydrogenated regions on the ND-H. The presence of sp^2-hybridized defect states may explain the limited CO_2 reduction activity of detonation hydrogenated NDs under DUV light compared to hydrogenated NDs with a higher crystallinity.[15] In the case of ND-O, the amount of surface sp^2 carbon is significantly reduced in the process of surface termination and therefore no such recombination is evidenced.

The emission of solvated electrons from ND-H upon VIS excitation can be explained by a combination of sp^2 graphitic islands and fully H-terminated surface areas. FLRs may enable light absorption while hydrogen-terminated functional groups offer favorable negative EA properties. Such an inhomogeneous electron emission model was first proposed by Cui *et al.* to explain sub-bandgap electron emission from diamond surfaces in vacuum.[21] Our work demonstrates that a similar process occurs on ND with much smaller sp^2-hybridized surface structures. We anticipate that by controlling more precisely the ratio between hydrogenated surface groups and FLRs content, the electron emission properties of ND-H under VIS light excitation could be further optimized. While sp^2-hybridized states function as intermediate states absorbing in the VIS region, other (mixed) covalent surface functionalization may be considered.[35] An essential aspect for efficient solvated electron emission would be to ensure a low-barrier electron transfer between the absorbing surface states/molecules and the electron-emitting surface groups to benefit most from the unique electronic properties of H-terminated diamond surfaces.

3 Conclusion

In summary, the early stages of the electron emission in water from NDs upon illumination with DUV and VIS light were probed using ultrafast TA spectroscopy. While the emission of solvated electrons was observed for hydrogenated, hydroxylated and carboxylated NDs upon DUV illumination, it was only detected for hydrogenated NDs upon VIS excitation. This is interpreted by synergistic effects between sp^2-hybridized carbon surface reconstructions, which serve as a pool of electrons to be excited with VIS light, and hydrogenated surface groups offering a local negative electron affinity facilitating electron emission. On the other hand, these FLRs are detrimental for electron emission upon DUV illumination as they behave as trap states increasing electron recombination. These findings may suggest that a mixed ND surface chemistry composed of hydrogenated surface groups for electron emission and visible-light absorbing states - sp^2-hybridized surface states in this work - should be considered for improving the electron emission properties of NDs and nanostructured diamond under solar excitation.

4 Acknowledgment

This work was supported by European Union's Horizon 2020 Research and Innovation program under Grant no. 665085 (DIACAT). CM acknowledges support by the German Federal Ministry of Education and Research's funding measure "CO2-WIN" (project "PRODIGY"). TK acknowledges the support of the Helmholtz Einstein International Berlin Research School in Data Science (HEIBRiDS). We thank the Zentral Einrichtung Datenverabeitung (ZEDAT) of Freie Universität Berlin for the allocation of computing resources.

5 Table of content

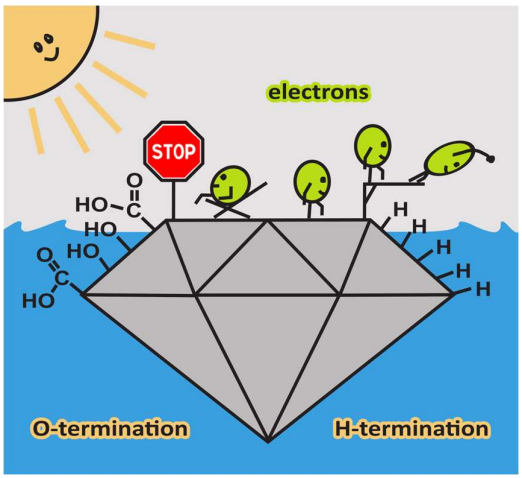

Ultrafast transient absorption reveals that solvated electrons are emitted in water upon illumination of nanodiamonds with deep ultraviolet or visible light. Synergistic effects between hydrogen termination and sp^2-hybridized surface reconstructions are evidenced to achieve electron emission through sub-bandgap light excitation.

References

[1] K. R. Siefermann, B. Abel, *Angewandte Chemie International Edition* **2011**, *50*, 5264–5272.

[2] J. A. Kloepfer, V. H. Vilchiz, V. A. Lenchenkov, A. C. Germaine, S. E. Bradforth, *The Journal of Chemical Physics* **2000**, *113*, 6288–6307.

[3] J. Stähler, J.-C. Deinert, D. Wegkamp, S. Hagen, M. Wolf, *Journal of the American Chemical Society* **2015**, DOI 10.1021/ja511571y.

[4] J. Stähler, C. Gahl, U. Bovensiepen, M. Wolf, *The journal of physical chemistry. B* **2006**, *110*, 9637–44.

[5] Y. Tong, F. Lapointe, M. Wolf, R. Kramer Campen, *Journal of the American Chemical Society* **2020**, *142*, 18619–18627.

[6] J. Zhao, B. Li, K. Onda, M. Feng, H. Petek, *Chemical Reviews* **2006**, *106*, 4402–4427.

[7] D. Zhu, L. Zhang, R. E. Ruther, R. J. Hamers, *Nature Materials* **2013**, *12*, 836–841.

[8] F. Maier, J. Ristein, L. Ley, *Physical Review B* **2001**, *64*, DOI 10.1103/PhysRevB.64.165411.

[9] M. Tomisaki, S. Kasahara, K. Natsui, N. Ikemiya, Y. Einaga, *Journal of the American Chemical Society* **2019**, *141*, 7414–7420.

[10] K. Natsui, H. Iwakawa, N. Ikemiya, K. Nakata, Y. Einaga, *Angewandte Chemie International Edition* **2018**, *57*, 2639–2643.

[11] D. Zhu, L. Zhang, R. E. Ruther, R. J. Hamers, *Nature materials* **2013**, *12*, 836–41.

[12] L. Zhang, D. Zhu, G. M. Nathanson, R. J. Hamers, *Angewandte Chemie International Edition* **2014**, *53*, 9746–9750.

[13] E. Brun, H. A. Girard, J.-C. Arnault, M. Mermoux, C. Sicard-Roselli, *Carbon* **2020**, *162*, 510–518.

[14] B. F. Bachman, D. Zhu, J. Bandy, L. Zhang, R. J. Hamers, *ACS Measurement Science Au* **2021**, DOI 10.1021/ACSMEASURESCIAU.1C00025.

[15] L. Zhang, R. J. Hamers, *Diamond and Related Materials* **2017**, *78*, 24–30.

[16] S. Li, J. A. Bandy, R. J. Hamers, *ACS Applied Materials & Interfaces* **2018**, *10*, 5395–5403.

[17] W. S. Yeap, X. Liu, D. Bevk, A. Pasquarelli, L. Lutsen, M. Fahlman, W. Maes, K. Haenen, *ACS Applied Materials & Interfaces* **2014**, *6*, 10322–10329.

[18] S. Choudhury, B. Kiendl, J. Ren, F. Gao, P. Knittel, C. Nebel, A. Venerosy, H. Girard, J.-C. Arnault, A. Krueger, K. Larsson, T. Petit, *Journal of Materials Chemistry A* **2018**, *6*, 16645–16654.

[19] S. Choudhury, R. Golnak, C. Schulz, K. Lieutenant, N. Tranchant, J.-C. Arnault, M.-A. Pinault-Thaury, F. Jomard, P. Knittel, T. Petit, *C* **2021**, *7*, 28.

[20] T. Sun, F. A. M. Koeck, C. Zhu, R. J. Nemanich, *Applied Physics Letters* **2011**, *99*, 202101.

[21] J. B. Cui, J. Ristein, L. Ley, *Physical Review B* **1999**, *60*, 16135–16142.

[22] P. Knittel, F. Buchner, E. Hadzifejzovic, C. Giese, P. Quellmalz, R. Seidel, T. Petit, B. Iliev, T. Schubert, C. Nebel, J. Foord, *ChemCatChem* **2020**, cctc.202000938.

[23] Y. Noda, C. Merschjann, J. Tarábek, P. Amsalem, N. Koch, M. J. Bojdys, *Angewandte Chemie International Edition* **2019**, *58*, 9394–9398.

[24] M. H. Elkins, H. L. Williams, A. T. Shreve, D. M. Neumark, *Science* **2013**, *342*, 1496–1499.

[25] A. Lübcke, F. Buchner, N. Heine, I. V. Hertel, T. Schultz, *Physical chemistry chemical physics : PCCP* **2010**, *12*, 14629–34.

[26] Y.-I. Suzuki, H. Shen, Y. Tang, N. Kurahashi, K. Sekiguchi, T. Mizuno, T. Suzuki, *Chemical Science* **2011**, *2*, 1094.

[27] T. Petit, L. Puskar, T. A. Dolenko, S. Choudhury, E. Ritter, S. Burikov, K. Laptinskiy, Q. Brzustowski, U. Schade, H. Yuzawa, M. Nagasaka, N. Kosugi, M. Kurzyp, A. Venerosy, H. A. Girard, J.-C. Arnault, E. Osawa, N. Nunn, O. Shenderova, E. F. Aziz, *The Journal of Physical Chemistry C* **2017**, *121*, 5185−5194.

[28] A. P. Gaiduk, T. A. Pham, M. Govoni, F. Paesani, G. Galli, *Nature Communications* **2018**, *9*, 247.

[29] M. Mermoux, A. Crisci, T. Petit, H. A. Girard, J.-C. Arnault, *Journal of Physical Chemistry C* **2014**, *118*, DOI 10.1021/jp507377z.

[30] G. Thalassinos, A. Stacey, N. Dontschuk, B. J. Murdoch, E. Mayes, H. A. Girard, I. M. Abdullahi, L. Thomsen, A. Tadich, J.-C. Arnault, V. N. Mochalin, B. C. Gibson, P. Reineck, *C* **2020**, *6*, 7.

[31] T. Petit, J.-C. C. Arnault, H. A. Girard, M. Sennour, T.-Y. Kang, C.-L. Cheng, P. Bergonzo, *Nanoscale* **2012**, *4*, 6792–9.

[32] P. Reineck, D. W. M. Lau, E. R. Wilson, K. Fox, M. R. Field, C. Deeleepojananan, V. N. Mochalin, B. C. Gibson, *ACS Nano* **2017**, *11*, 10924–10934.

[33] C. Bannwarth, E. Caldeweyher, S. Ehlert, A. Hansen, P. Pracht, J. Seibert, S. Spicher, S. Grimme, *WIREs Comput. Mol. Sci.* **2021**, *11*, e1493.

[34] A. Bolker, C. Saguy, M. Tordjman, R. Kalish, *Physical Review B* **2013**, *88*, 035442.

[35] I. Boukahil, P. S. Johnson, F. J. Himpsel, R. Qiao, J. A. Bandy, R. J. Hamers, *Journal of Vacuum Science & Technology A* **2017**, *35*, 04D102.